Biosensors and Bioelectronics 185 (2021) 113241

Contents lists available at ScienceDirect

Biosensors and Bioelectronics

journal homepage: http://www.elsevier.com/locate/bios

Highly sensitive detection of malignant glioma cells using metamaterial-inspired THz biosensor based on electromagnetically induced transparency

Jin Zhang [a,1], Ning Mu [b,c,1], Longhai Liu [d,e], Jianhua Xie [e], Hua Feng [b,c], Jianquan Yao [d], Tunan Chen [b,c,**], Weiren Zhu [a,*]

[a] Department of Electronic Engineering, Shanghai Jiao Tong University, Shanghai, 200240, China
[b] Department of Neurosurgery, Southwest Hospital, Army Medical University (Third Military Medical University), Chongqing, 400038, China
[c] Collaborative Innovation Center for Brain Science, Chongqing, China
[d] Tianjin University, Tianjin, 300072, China
[e] Advantest (China) Co., Ltd, Shanghai, 201203, China

ARTICLE INFO

Keywords:
Biosensing
Metamaterials
THz
Cancer detection

ABSTRACT

Metamaterial-inspired biosensors have been extensively studied recently years for fast and low-cost THz detection. However, only the variation of the resonance frequency has been closely concerned in such sensors so far, whiles the magnitude variation, which also provide important information of the analyte, has not been sufficiently analyzed. In this paper, by the observation of two degree of variations, we propose a label-free biosensing approach for molecular classification of glioma cells. The metamaterial biosensor consisting of cut wires and split ring resonators are proposed to realize polarization-independent electromagnetic induced transparency (EIT) at THz frequencies. Simulated results show that the EIT-like resonance experiences both resonance frequency and magnitude variations when the properties of analyte change, which is further explained with coupled oscillators model theory. The theoretical sensitivity of the biosensor is evaluated up to 496.01 GHz/RIU. In experiments, two types of glioma cells (mutant and wild-type) are cultured on the biosensor surface. The dependences of frequency shifts and the peak magnitude variations on the cells concentrations for different types give new perspective for molecular classification of glioma cells. The measured results indicate that the mutant and wild-type glioma cells can be distinguished directly by observing both the variations of EIT resonance frequency and magnitude at any cells concentrations without antibody introduction. Our metamaterial-based biosensor shows a great potential in the recognition of molecule types of glioma cells, opening alternative way to sensitive biosensing technology.

1. Introduction

Gliomas are the most common malignant intracranial tumors with rapid growth, high invasiveness, and poor prognosis Asthagiri et al. (2007); Gilbertson and Rich (2007); Omuro and DeAngelis (2013). Recently, the understanding and treatment of gliomas have been significantly changed by the discovery of mutations involving the isocitrat edehydrogenase (IDH) enzymes Sun et al. (2013). Researchers found that the patients of gliomas with a mutation in the IDH gene have higher survival rate than those of wild-type cases. Rapid and accurate early detection is extremely important for the diagnosis and treatment of malignant gliomas. Hematoxylin and eosin-stained histological biopsy is the current rapid intraoperative diagnosis mean of glioma Asthagiri et al. (2007); Chen et al. (2017). However, the strong dependence on the subjective judgment of brain surgeons only enables tumors morphological observation and pathological grade determination. Owing to the advantages of high precision and selectivity, bio-labeling techniques including enzyme linked immunosorbent assay Kirnbauer et al. (1994),

* Corresponding author.
** Corresponding author. Department of Neurosurgery, Southwest Hospital, Army Medical University (Third Military Medical University), Chongqing, 400038, China.
E-mail addresses: ctn@tmmu.edu.cn (T. Chen), weiren.zhu@sjtu.edu.cn (W. Zhu).
[1] These authors contributed equally to this work and should be considered co-first authors.

https://doi.org/10.1016/j.bios.2021.113241
Received 4 February 2021; Received in revised form 6 April 2021; Accepted 7 April 2021
Available online 22 April 2021
0956-5663/

radioimmunoassay Bast et al. (1983), and immunohistochemistry Zaha (2014) have been applied in clinic to achieve glioma cell molecular typing. Although all these techniques are efficient, they are associated with major limitations including being time consuming and expensive while require well-trained personnel as well as restrictive experimental conditions. Therefore, it is necessary to develop a rapid, high-sensitive and yet simple cell detection method for the diagnosis of glioma tumors, which would be extremely useful for identifying the intra-operative glioma molecular types and guiding doctors to formulate more accurate clinical treatment strategies.

In recent years, biosensing technology opens up new opportunities for high-sensitive detection of cancer cells. Owing to the well-established micromachining techniques, various biosensors have been proposed based on the principle of surface plasmonic resonance Hu et al. (2006); Lertvachirapaiboon et al. (2018), interferometric Bast et al. (1983), as well as optrode-based fiber Quero et al. (2016). Recently, the rapid development of terahertz (THz) technology is ushering in a tantalizing feasibility for another label-free and non-invasive biosensor approach Yu et al. (2012); Menikh et al. (2004); Yang et al. (2016); Wallace et al. (2006). THz radiation has quite low photon energy effectively avoiding harmful ionization to biomolecules and can excite low-frequency intermolecular interactions, including hydrogen bonds, van der Waals and framework vibration. However, due to the weak interaction between THz waves and natural materials, THz spectroscopy commonly has poor sensitivity in practical applications. To improve the sensitivity, various efforts have been devoted to exploring unconventional sensing techniques with the utilization of electromagnetic metamaterials. Metamaterials are composed of artificial periodic subwavelength structures and have extraordinary properties that not available in natural materials, which become a powerful tool for the manipulation of electromagnetic waves and their interaction with matters Chen et al. (2006, 2012); Landy et al. (2008); Salim and Lim (2018). For examples, Rodrigo et al. exploited the unique electro-optical properties of graphene based metamaterial to demonstrate a tunable plasmonic biosensor for chemical label-free detection of protein monolayers Rodrigo et al. (2015). The concept of electromagnetic induced transparency (EIT) which refers to an extremely narrowband transparency window has been introduced in metamaterials providing a potential way to achieve ultrasensitive sensor in the THz region Papasimakis et al. (2008); Yang et al. (2014); Tassin et al. (2012); He et al. (2017); Wei et al. (2017). Liu et al. (2010) demonstrated a complementary metamaterial sensor based on EIT at optical frequencies, yielding a high sensitivity for refractive index. Yan et al. (2019) experimentally proposed an EIT-like biosensor for detection of oral cancer cells (HSC3), showing maximum sensitivity of 900 kHz/cell ml^{-1}. Later on, Yang et al. (2019) experimentally achieved analogous detection of lung cancer cells based on an EIT metamaterial. However, in all these metamaterial-inspired sensing techniques, only the frequency shifts induced by the refractive index of the analyte are monitored, while the magnitude responses, another significant characteristic of the sensors, have not been sufficiently analyzed. By examining both the frequency and magnitude variations, metamaterial sensors may perform more fruitful functions in practical applications. Furthermore, it is unavoidable to work with unpolarized terahertz beam in practical biological detection, and the polarization state of incident THz wave may change after passing through different layers of analytes. Therefore, the polarization-independent metamaterials are essential for application in terahertz biosensing.

In this paper, we propose an EIT metamaterial biosensor for highly sensitive detection and quick molecular typing of glioma cells, offering neurosurgeons the accurate clinical treatment strategy for malignant glioma tumors. The proposed EIT metamaterial consists of metallic cut wires and split ring resonators (SRRs), which enables to generate a polarization-independent transparency window at 2.24 THz. Such a metamaterial sensor shows potentials for quantitative concentration detection and qualitative molecule type identification. As the proof of concept, two types of glioma cells (mutant, wild-type) are cultured and adhered on the metal surface of the proposed metamaterial biosensor. By measuring the THz transmission spectra, both frequency and magnitude responses for different concentrations of cells are obtained. The maximum experimental sensitivity can approach 248.75 kHz/cell ml^{-1} at 8$\times$ 10^5 cells/ml for wild-type glioma cell. More critically, the dependence of the resonance frequency shift and peak magnitude variation on cell concentrations enable to directly distinguish different types of cells without any antibody introduction and cellular staining. Such novel EIT-like biosensors exhibit promising potentials for future biological detection of glioma cells.

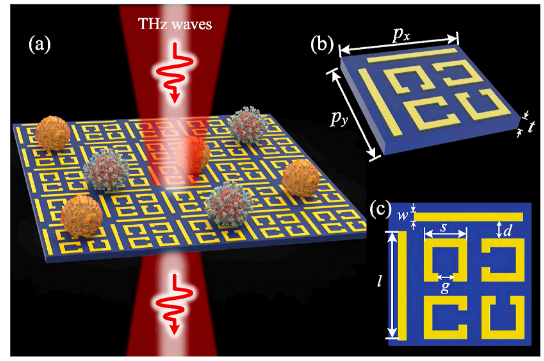

Fig. 1. a) Schematic illustration of the proposed metamaterial biosensor: THz beams normally penetrate through the devices on which different types of cells were cultured. b) and c) The structural configuration and the top view of unit cell consisting of metal patterns and substrate, respectively. The structure parameters are listed as: $p_x = p_y = 50\mu$m, $l = 38\mu$m, $w = 3\mu$m, $s = 15\mu$m, $g = 5\mu$m, $d = 6\mu$ m and.$\varepsilon = 3.85$

2. Simulation and experimental method

The schematic illustration and geometric parameters of our proposed metamaterial biosensor are shown in Fig. 1. The unit cells of resonant metamaterial are arranged in a periodical array and the substrate is adopted as 500μm-thick quartz glass ($\varepsilon = 3.85$). Full-wave numerical simulations are performed using the commercial software CST Microwave studio. In simulations, periodical boundary conditions with Floquet-port are employed in the x- and y-directions and open (add space) boundary conditions are utilized in the z direction along the propagation of the incident plane wave.

The proposed biosensor samples were fabricated by standard photolithography technology followed by the deposition of 10 nm chromium and 100 nm gold. It is noted that the chromium layer is used for adhesion in fabrication. In simulations, the chromium and gold are modelled as lossy metals with the conductivities of 8×10^6 S/m and 4.561×10^7 S/m, respectively. The optical microscope image of the fabricated biosensor sample is shown in Fig. 2(a–c), which has 100 unit cells along both the x- and y-directions. The whole physical dimension of the metallic array is 5 mm $\times$ 5 mm. In order to verify the performance of the proposed biosensor, mutant glioma cells (U87$^{\mathrm{IDH-}}$) and wild-type glioma cells (U87) were chosen as analytes. The two types of glioma cells are cultured in Dulbecco's modified Eagle medium (DMEM) containing 10 % fetal bovine serum and 10% penicillin streptomycin (both from Gibco) at 37 °C with 5% CO_2 in a humidified atmosphere. Then, the adherent cells were collected by a series of biological operations [digesting with trypsin-EDTA (Gibco), centrifugal treatment and counting the cell numbers]. After the proposed biosensor were sterilized with 75 % ethanol, a cell suspension of a certain concentration was seeded on the surface of the biosensor and cultured again at the environment mentioned before. Fig. 2(e–g) show the micrographs of the fabricated biosensor cultured with different cells concentrations. Before measurement, the fabricated biosensor was washed twice with

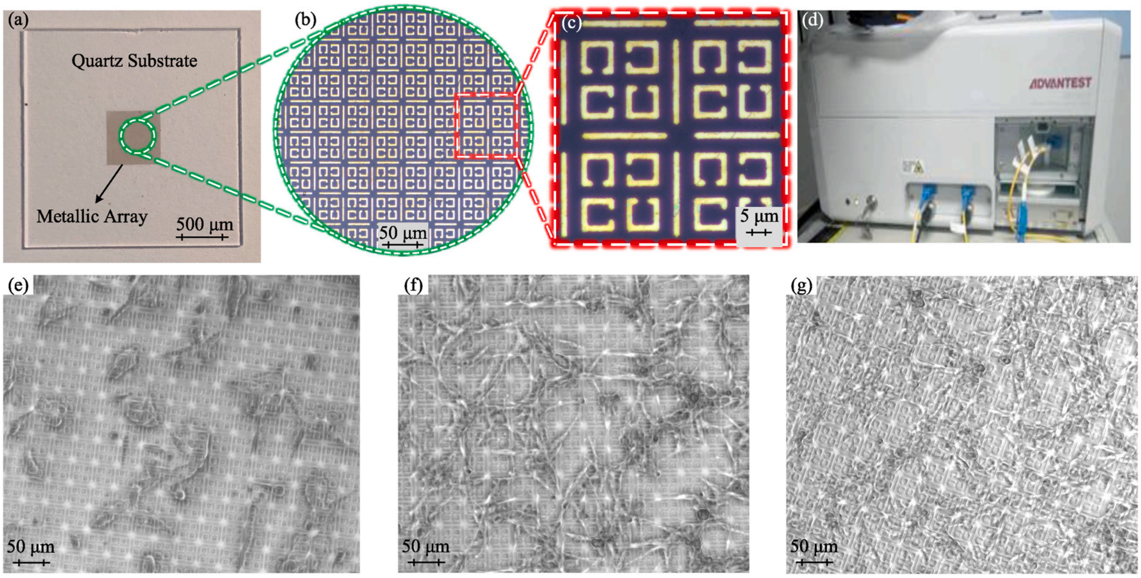

Fig. 2. a) Physical photograph of the proposed biosensor. b) and c) Photomicrograph of the fabricated metasurface in a small zone. d) The measurement setup. The micrograph of glioma cells adhered on metamaterial surface with the concentration of e) 20×10^4 cells/mL, f) 60×10^4 cells/mL and g) 80×10^4 cells/mL, respectively.

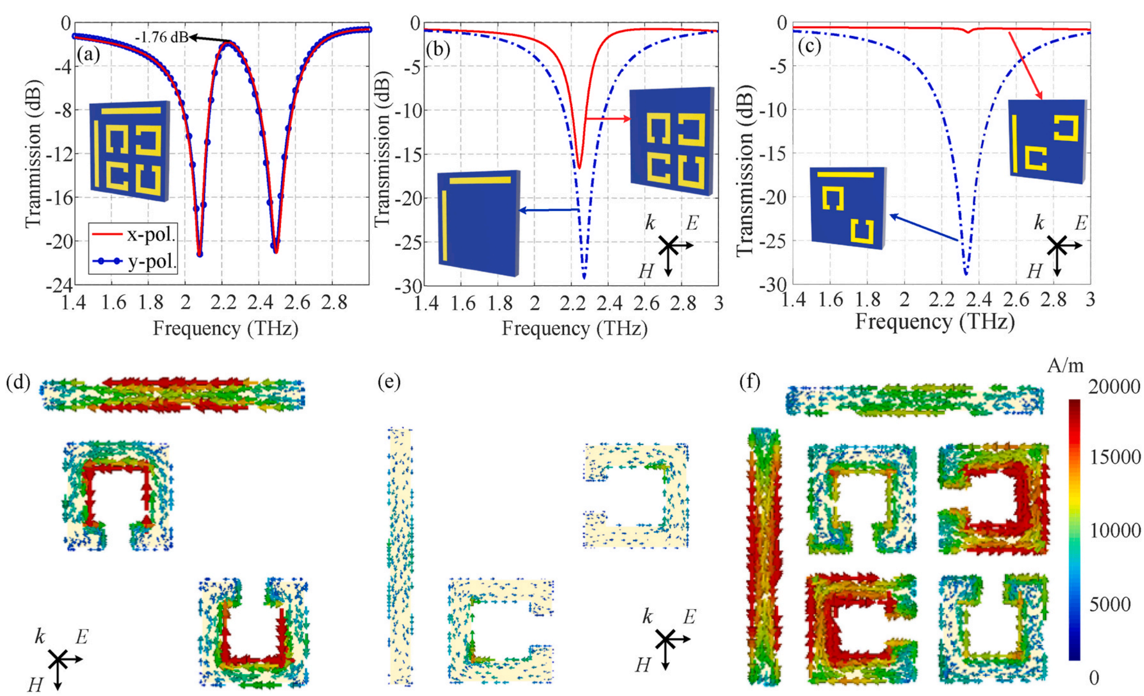

Fig. 3. a) Simulated transmission spectra of the EIT-like metamaterial under x- and y-polarized incident wave. b) Simulated transmission spectra of SRRs and cut wires. c) Simulated transmission spectrum of bright mode (blue line) and dark mode (red line). The surface currents distribution of d) bright mode, e) dark mode and f) whole metamaterial at 2.24 THz. (For interpretation of the references to colour in this figure legend, the reader is referred to the Web version of this article.)

phosphate-buffered saline, followed by drying treatment using blotting papers.

As shown in Fig. 2(d), the THz transmission spectra of the biosensor samples were measured by applying a commercial THz-TDS system (Advantest TAS7500SP), with the spectral resolution of 7.6 GHz. The effective frequency region ranges from 0.1 to 4.0 THz. After the cells culture and pre-preparation, the biosensors were fixed on the sample holders in the THz-TDS system, which were perpendicular to the connecting line between the radiation transmitter and detector. The THz transmission spectra of the biosensor covered with glioma cells were detected at room temperature of 26 °C and a relative humidity below 3%. The time domain data of the measured spectra were converted into frequency domain data based on Fourier transform and then normalized the transmission values with the reference of air.

3. Results and discussion

Fig. 3(a–c) exhibit the simulated transmission spectra of the proposed metamaterial biosensor, as well as the results for cut wires and SRRs. It is seen in Fig. 3(b) that the both cut wires and SRRs can be

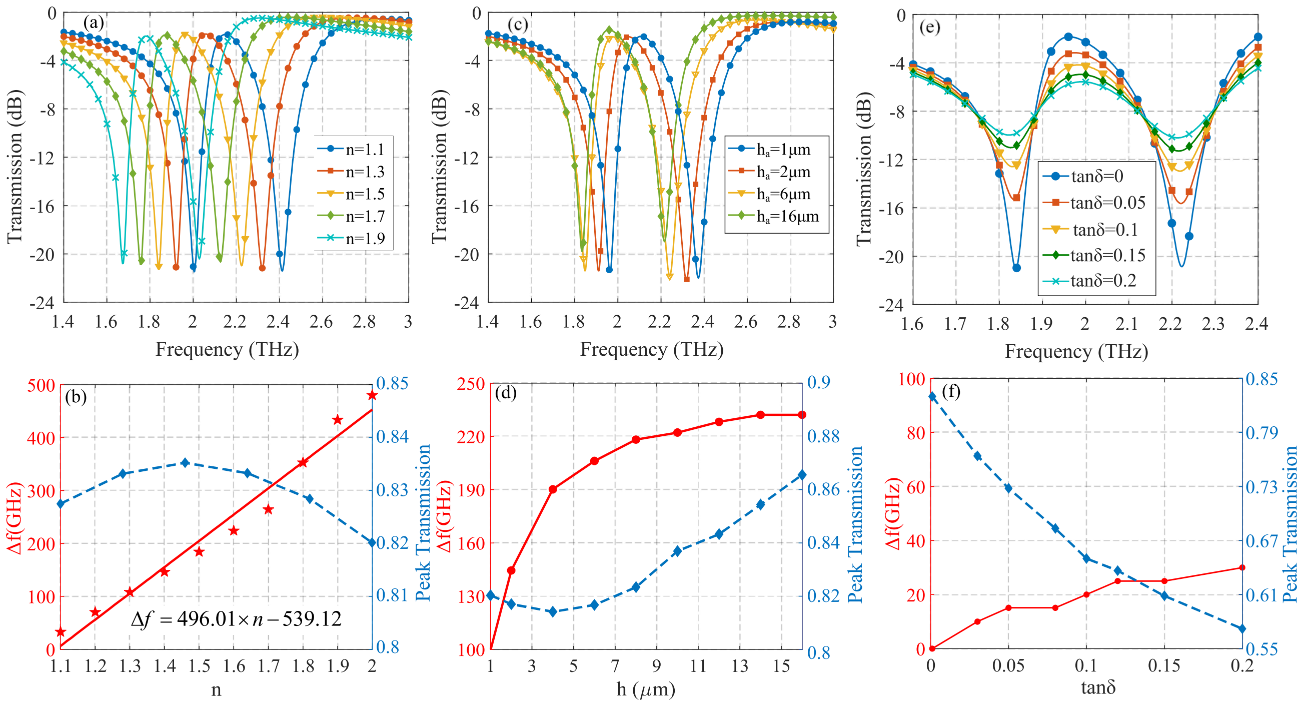

Fig. 4. a) The simulated transmission spectra of the proposed biosensor covered by 10 μm-thick analyte with the refractive index increasing from 1.1 to 1.9. b) The relations between frequency shift (peak transmission) and the refractive index of the analyte. c) The dependence of transmission on the analyte thickness increasing from 1 to 16 μm under the fixed refractive index of 1.6. d) The relations between frequency shift (peak transmission) and the thickness of the analyte. e) The dependence of transmission on the loss tangent of the analyte increasing from 0 to 0.2. f) The relations between frequency shift (peak transmission) and the loss tangent of the analyte.

excited by x-polarized incident waves and their resonant frequencies are nearly equal to 2.24 THz. Then the horizontal cut wire together with two diagonal SRRs whose gap is perpendicular to the direction of the incident polarization are defined as a narrow bright mode while the other structures are defined as a broad dark mode. Fig. 3(c) shows that the bright mode alone generates a strong resonance with high Q factor. In contrast, the dark mode has weak interaction with the incident wave, generating a lower Q factor resonance. When the bright and dark modes are put together, the two resonances destructively interfere with each other, resulting in a narrow transparency between two transmission dips. In Fig. 3(a), we show the transmission spectra under x- or y-polarized incident waves are well overlapped, indicating the polarization independence of the proposed metamaterial due to its four-fold rotational symmetry. It is also seen that the peak transmission of EIT spectrum is about -1.76 dB (67%) and the energy is mainly consumed by the losses of the metal resonators. A narrower EIT spectrum typically means a higher Q-factor of the resonance, and thus higher field enhancement around the metamaterial. As a result, it will be more sensitive to the environment changes, showing higher sensitivity of the EIT spectrum. On the other hand, the transmission of EIT will reduce when increasing the Q value of the metamaterial due to the metal losses of resonators. Hence, the design of our proposed metamaterial is a perfect trade-off between high Q-factor and low energy losses. In order to further investigate the physical mechanism of the EIT resonance, the surface current distributions of bright mode, dark mode, and the entire metamaterial at 2.24 THz are plotted in Fig. 3 (d-f). As shown in Fig. 3 (d), when an x-polarized THz wave is incident on the bright mode alone, a strong enhancement of surface currents is directly excited concentrating on the horizontal cut wire and the inner side of SRRs. In contrast, the vertical cut wire and other two diagonal SRRs scarcely show any responses to the x-polarized incidence. By combining the cut wires with the two pairs of SRRs to form a whole unit cell, the strong surface current enhancement entirely transfers to the dark mode resonator through the near field coupling with the bright mode resonator, and obvious circulated surface charges along the SRRs whose gaps are parallel to the direction of incident electric fields, indicating an induced magnetic dipole on dark mode with small radiative loss. Since the strength of the indirect resonance of the dark mode is comparable to that of the direct resonance of the bright mode, the destructive interference between them gives rise to the narrow transparency window at 2.24 THz.

In order to explore the sensitivity of the metamaterial sensor, we first evaluated the refractive index sensing performance by numerical simulations. In the simulation, an analyte layer with a thickness of $h_a = 10\mu m$ was added onto the metamaterial. Fig. 4(a) illustrates that when the refractive index of the analyte increases from 1.1 to 1.9, the transparency peak experiences an obvious red-shift in frequency and insignificant variation in magnitude. The working frequency of EIT effect is determined by the resonant structure and surrounding dielectric medium. When covering the analyte with high refraction index onto the top surface of metal resonators, the equivalent dielectric constant of surrounding medium increases correspondingly which leads to the variation of induced electric fields and eventually shifts the central peak. The related frequency shift Δf and absolute peak transmission under different refractive index n were displayed in Fig. 4(b). We can see a nearly linear relationship between the frequency shift Δf and the refractive index n. In addition, owing to the high Q value of EIT effect, the theoretical sensitivity of the proposed biosensor can be calculated as $S = \Delta f / \Delta n \approx 496.01$ GHz/RIU which is sensible in practical application.

We further studied the influence of the thickness of the analyte on the proposed metamaterial biosensor. Fig. 4(c) and (d) show the moving tendency of the THz spectra under different thicknesses of the analyte h_a when the refractive index is set to 1.6. It can be seen that the proposed biosensor is sensitive to the thickness of the analyte, and the frequency shift Δf increases with the increase of h_a. Furthermore, the relationship between Δf and h_a shows that the frequency of the transparency peak shifts significantly when the thickness varies from $1\mu m$ to $8\mu m$ and

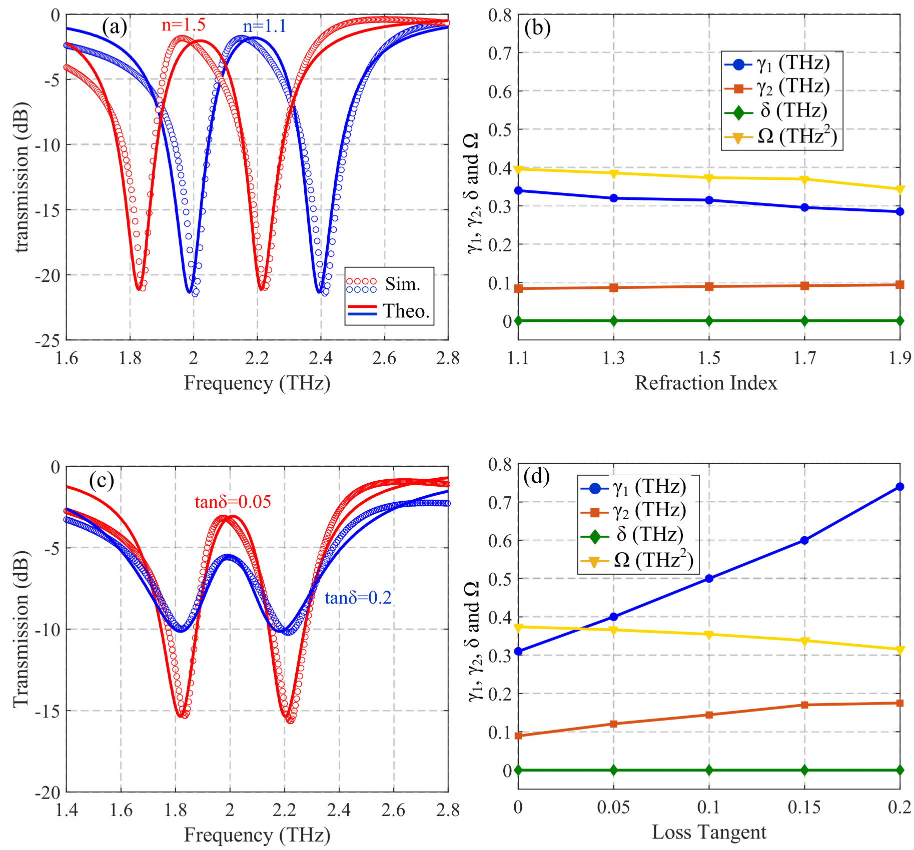

Fig. 5. The fitting theory results of coupled harmonic oscillator model to simulated transmission spectra with different a) refractive index and c) loss tangent. b) The dependence of γ_1, γ_2, δ and Ω extracted by fitting the transmission curves on b) refractive index and d) loss tangent, respectively. The unit of Ω is THz^2.

almost keeps unchanged when the thickness reached 14μm. This is because the excited-field and the coupling effect of the metal structure is localized on its surface area.

Besides, the dielectric loss of the analyte can also affect the EIT-like transmission spectrum of the proposed biosensor. Here, the loss tangent (tanδ) is used to characterize the dielectric loss of the analyzed cells in simulations. From Fig. 4(e) and (f), it is seen that when the loss tangent increases from 0 to 0.2 under the fixed refractive index of 1.6 and thickness of 10μm, the frequency shift Δf changes slightly while the peak transmission magnitude reduces significantly from 0.83 to 0.57. Compared with the other cases shown in Fig. 4(b),(d) and (f), it can be concluded that the dielectric loss is the most sensitive factor that affecting the magnitude of EIT-like transmission peak. Such a feature offers a new degree of freedom for applications in bio-molecule detection.

In order to reveal the physical mechanism of the proposed EIT metamaterial, a coupled harmonic oscillator model is employed to quantitatively describe the near field coupling between the bright and dark mode resonators. The concept of EIT is derived from a media transparent phenomenon in the three-level atomic system Boller et al. (1991). The interference in the proposed metamaterial can be described by the coupled differential equations Gu et al. (2012); Meng et al. (2012):

$$\ddot{x}_1 + \gamma_1\dot{x}_1 + \omega_0^2 x_1 + \Omega x_2 = gE_0 e^{j\omega t},$$
$$\ddot{x}_2 + \gamma_2\dot{x}_2 + (\omega_0 + \delta)^2 x_2 + \Omega x_1 = 0, \quad (1)$$

where x_1, x_2, γ_1 and γ_2 represent the magnitudes and losses of the bright and dark mode resonances, respectively. ω_0 is the resonance frequency of the bright mode oscillator ($\gamma_2 \ll \gamma_1 \ll \omega_0$), δ and Ω represent the frequency detuning factor and coupling coefficient between the dark mode and bright mode oscillators ($\delta \ll \gamma_1$). g is a geometric parameter indicating the coupling strength of the of the bright mode resonator with the source field $E_0 e^{j\omega t}$. Under the condition of $\omega - \omega_0 \ll \omega_0$ and $\omega_0^2 - \omega^2 \approx -2\omega_0(\omega - \omega_0)$ Liu et al. (2009), the susceptibility χ of the EIT metamaterial can be derived as Luo et al. (2016):

$$\chi = \chi_r + i\chi_i \propto \frac{(\omega - \omega_0 - \delta) + \frac{i\gamma_2}{2}}{\left(\omega - \omega_0 + \frac{i\gamma_1}{2}\right)\left(\omega - \omega_0 - \delta + \frac{i\gamma_2}{2}\right) - \frac{\Omega^2}{4}} \quad (2)$$

Due to the ultrathin thickness of metal resonators and the large mismatch of the wave vector between the metamaterial and far-field, the scattering of incident waves is very weak and most of the energies are dissipated in the EIT system. Therefore, the energy loss is always proportional to the imaginary part of χ, and therefore the transmittance T can be written as: $T \propto 1 - \chi_i = 1 - g\chi_i$. Ding et al. (2014); Xiao et al. (2018) As shown in Fig. 5(a) and (c), the transmission spectra of the proposed EIT-like metamaterial are theoretically fitted according to the coupled harmonic oscillator model, exhibiting a good consistency with the CST simulation results. The related fitting parameters as a function of the refractive index and the loss tangent of the analyte are shown in Fig. 5(b) and (d), respectively. It is seen in Fig. 5(b) that δ and γ_2 are almost constant while γ_1 and Ω reduce slightly with the increasing of the refraction index. In Fig. 5(d), both γ_1 and γ_2 experience significant growth with the increasing of the loss tangent of the analyte while Ω decreases slightly from 0.38 to 0.32 THz. The results in Fig. 5 demonstrate that the physical properties of the analyte may affect the local field on the surface of the EIT-like metamaterial, thus changing the self and mutual coupling between bright and dark modes. Therefore, both the frequency and magnitude variation of the EIT peak occur in the transmission spectra, offering significant potential for sensing applications.

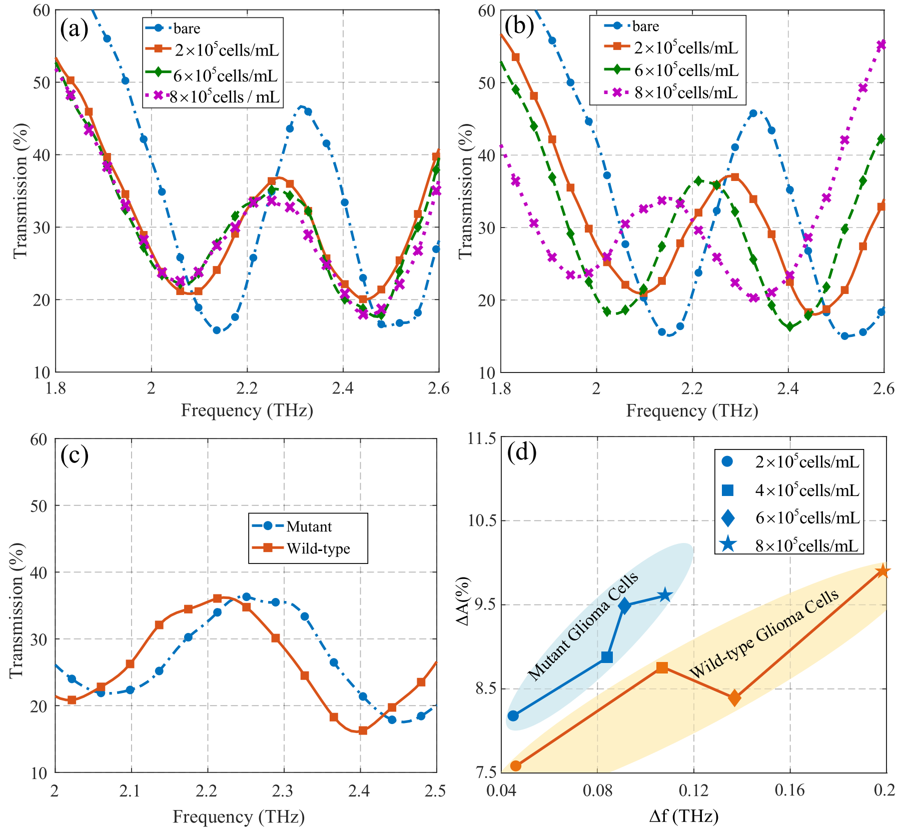

Fig. 6. The measured transmission spectra of the proposed biosensor covered by a) the mutant IDH glioma cells and b) the wild-type IDH glioma cells. c) The measured transmission spectra of twotypes of cells with same cells concentration of 4×10^5 cells/mL. d) The resonate frequency shifts and the peak magnitude variations for mutant and wild-type glioma cells as the concentration changes.

The practical performances of the EIT-like metamaterial for biosensing are experimentally studied. Two types of glioma cells are cultured onto the surface of the metamaterial. First, we investigate the ability of the proposed biosensor to detect the variation of cell concentrations. Fig. 6(a–b) show the measured THz spectra of the proposed biosensor covered by mutant or wild-type glioma cells with different concentrations. The THz spectra of bare samples are also provided for comparison. It is seen that the transmission spectra of both types of glioma cells experience obvious variations on the resonant frequency and peak magnitude. For example, when the concentration of mutant glioma cells raises from 2×10^5 cells/mL to 8×10^5 cells/mL, the resonant frequency shifts from 2.274 THz to 2.228 THz while the peak magnitude slightly reduces from 36.73% to 34.21%. Similar trends are found in the wild-type glioma cells. The practical sensitivity in experiment is defined as $S = \Delta f / \Delta c$, where Δc is the variation of the cell concentration. The maximum sensitivities for the mutant and wild-type glioma cells are accordingly calculated as 122 kHz/cell ml^{-1} and 248.75 kHz/cell ml^{-1}, respectively. These results demonstrate that the proposed EIT-like metamaterial is a promising platform for the sensitive detection of the glioma cells from physical perspective. The difference between the simulated and measured sensitivity is due to the slight changes of cells' refractive index and the noises from the measurement environment.

Subsequently, the ability of the proposed biosensor to distinguish different types of cells is studied. Fig. 6(c) shows the measured THz spectra of the biosensor covered by mutant or wild-type glioma cells at the same concentration of 4×10^5 cells/mL. It is seen that the resonant frequencies of the two types of glioma cells are obviously different. The measured results indicate that the proposed biosensor successfully realize the recognition of cancer cells at the specific cells concentration. However, it's time-consuming to culture sample with specific cells concentration in practical detection. In order to recognize molecular types of the glioma cells efficiently, the frequency shift combined with the peak magnitude variation are evaluated simultaneously and their dependences on concentrations for mutant and wild-type glioma cells are illustrated in Fig. 6(d). It is seen that for the wild-type glioma cells, the variation of cells concentration leads to the resonance frequency shift nearly up to 0.2 THz. While for the mutant glioma cells, the frequency shift is only 0.12 THz and the concentration changes are mainly reflected in peak magnitude variation. Moreover, the two polylines in Fig. 6(d) are separated with each other, indicating the variation regions of frequency and magnitude for mutant cells (blue zone) and wild-type glioma cells (yellow zone). This clearly shows that once two degrees of variations are measured, the type of the glioma cells as well as its concentration can be directed read from Fig. 6(d). It is worth noting that two types of glioma cells have different water content and nuclear size, which results in the differences in both the refractive index and dielectric loss. As theoretically analyzed in Fig. 4, the variations of resonance frequency and magnitude in the proposed metamaterial sensor are highly related to the refractive index and dielectric loss of the analytes. Although the proposed biosensor is only designed for distinguishing the specific types of target cells at present, the experimental results demonstrate the significant potentials in practical application of glioma molecular classification, offering a new route for the fast and low-cost detection for cancer cells.

4. Conclusion

In this paper, we have proposed a novel biosensing technology based on polarization-independent metamaterials for molecular classification of glioma cells. A metamaterial biosensor composed of SRRs and cut wires was designed, which induced an EIT-like resonant peak at 2.24 THz. The corresponding electric fields and surface current distributions verify that the EIT-like phenomenon is attributed to coupling and the destructive interference between bright mode and dark mode. The coupled harmonic oscillator model was used to reveal the physical mechanism of the EIT effect. In simulation, it is found that resonant frequency of the proposed biosensor experiences a red shift with the increase of the analyte's refractive index. The corresponding theoretical sensitivity of the biosensor is calculated up to 496.01 GHz/RIU. Moreover, we also investigated the variation of peak magnitude which depends on the dielectric loss of the analyte. Such characteristics are of great benefit to the cell detection. In experiments, two types of glioma cells (mutant and wild type) are cultured on the surface of the proposed biosensor with different cells concentrations. The maximum experimental sensitivity approaches 248.75 kHz/cell ml^{-1} which enables sensitive detection of the glioma cells activity from physical perspective. Furthermore, the resonate frequency shift combined with peak magnitude variation were evaluated simultaneously. The measured results demonstrated that their dependence on cell concentration are quite different between mutant and wild-type glioma cells, which can account for the glioma tissue discrimination. Therefore, the proposed biosensor shows the significant potentials in the application of glioma molecular classification and also offers a novel way to obtain the fast and low-cost cells detection.

CRediT authorship contribution statement

Jin Zhang: Investigation, Methodology, Software, Data curation, Visualization, Writing – original draft, preparation. **Ning Mu:** Investigation, Methodology, Formal analysis, Validation. **Longhai Liu:** Resources, Writing – review & editing. **Jianhua Xie:** Resources, Project administration. **Hua Feng:** Project administration, Resources. **Jianquan Yao:** Supervision, Writing – review & editing, Project administration. **Tunan Chen:** Supervision, Writing – review & editing. **Weiren Zhu:** Conceptualization, Supervision, Writing – review & editing.

Declaration of competing interest

The authors declare that they have no known competing financial interests or personal relationships that could have appeared to influence the work reported in this paper.

Acknowledgements

This work was supported by the National Natural Science Foundation of China (NSFC) (62071291 and 51777168) and Talents Training Program of Army Medical University (2019MPRC021).

References

Asthagiri, A.R., Pouratian, N., Sherman, J., Ahmed, G., Shaffrey, M.E., 2007. Advances in brain tumor surgery. Neurol. Clin. 25, 975–1003. Brain Tumors in Adults.

Bast, R.C., Klug, T.L., John, E.S., Jenison, E., Niloff, J.M., Lazarus, H., Berkowitz, R.S., Leavitt, T., Griffiths, C.T., Parker, L., Zurawski, V.R., Knapp, R.C., 1983. A radioimmunoassay using a monoclonal antibody to monitor the course of epithelial ovarian cancer. N. Engl. J. Med. 309, 883–887.

Boller, K.J., Imamoğlu, A., Harris, S.E., 1991. Observation of electromagnetically induced transparency. Phys. Rev. Lett. 66, 2593–2596.

Chen, H.T., Padilla, W.J., Zide, J.M., Gossard, A.C., Taylor, A.J., Averitt, R.D., 2006. Active terahertz metamaterial devices. Nature 444, 597–600.

Chen, J.M., Li, Y., Xu, J., Gong, L., Wang, L.W., Liu, W.L., Liu, J., 2017. Computer-aided prognosis on breast cancer with hematoxylin and eosin histopathology images: a review. Tumor Biol. 39, 1010428317694550.

Chen, T., Li, S., Sun, H., 2012. Metamaterials application in sensing. Sensors 12, 2742–2765.

Ding, J., Arigong, B., Ren, H., Zhou, M., Shao, J., Lu, M., Chai, Y., Lin, Y., Zhang, H., 2014. Tuneable complementary metamaterial structures based on graphene for single and multiple transparency windows. Sci. Rep. 4, 1–7.

Gilbertson, R.J., Rich, J.N., 2007. Making a tumour's bed: glioblastoma stem cells and the vascular niche. Nat. Rev. Canc. 7, 733–736.

Gu, J., Singh, R., Liu, X., Zhang, X., Ma, Y., Zhang, S., Maier, S.A., Tian, Z., Azad, A.K., Chen, H.T., et al., 2012. Active control of electromagnetically induced transparency analogue in terahertz metamaterials. Nat. Commun. 3, 1–6.

He, X., Yang, X., Lu, G., Yang, W., Wu, F., Yu, Z., Jiang, J., 2017. Implementation of selective controlling electromagnetically induced transparency in terahertz graphene metamaterial. Carbon 123, 668–675.

Hu, W., Hsu, H.Y., Chiou, A., Tseng, K., Lin, H.Y., Chang, G., Chen, S.J., 2006. Immunodetection of pentamer and modified c-reactive protein using surface plasmon resonance biosensing. Biosens. Bioelectron. 21, 1631–1637.

Kirnbauer, R., Hubbert, N.L., Wheeler, C.M., Becker, T.M., Lowy, D.R., Schiller, J.T., 1994. A virus-like particle enzyme-linked immunosorbent assay detects serum antibodies in a majority of women infected with human papillomavirus type 16. JNCI: J. Natl. Cancer Inst. 86, 494–499.

Landy, N.I., Sajuyigbe, S., Mock, J.J., Smith, D.R., Padilla, W.J., 2008. Perfect metamaterial absorber. Phys. Rev. Lett. 100, 207402.

Lertvachirapaiboon, C., Baba, A., Ekgasit, S., Shinbo, K., Kato, K., Kaneko, F., 2018. Transmission surface plasmon resonance techniques and their potential biosensor applications. Biosens. Bioelectron. 99, 399–415.

Liu, N., Langguth, L., Weiss, T., Kästel, J., Fleischhauer, M., Pfau, T., Giessen, H., 2009. Plasmonic analogue of electromagnetically induced transparency at the drude damping limit. Nat. Mater. 8, 758–762.

Liu, N., Weiss, T., Mesch, M., Langguth, L., Eigenthaler, U., Hirscher, M., Sönnichsen, C., Giessen, H., 2010. Planar metamaterial analogue of electromagnetically induced transparency for plasmonic sensing. Nano Lett. 10, 1103–1107.

Luo, W., Cai, W., Xiang, Y., Wang, L., Ren, M., Zhang, X., Xu, J., 2016. Flexible modulation of plasmon-induced transparency in a strongly coupled graphene grating-sheet system. Opt Express 24, 5784–5793.

Meng, F., Wu, Q., Erni, D., Wu, K., Lee, J., 2012. Polarization-independent metamaterial analog of electromagnetically induced transparency for a refractive-index-based sensor. IEEE Trans. Microw. Theor. Tech. 60, 3013–3022.

Menikh, A., Mickan, S.P., Liu, H., MacColl, R., Zhang, X.C., 2004. Label-free amplified bioaffinity detection using terahertz wave technology. Biosens. Bioelectron. 20, 658–662. Optical Biosensing.

Omuro, A., DeAngelis, L.M., 2013. Glioblastoma and other malignant gliomas: a clinical review. Jama 310, 1842–1850.

Papasimakis, N., Fedotov, V.A., Zheludev, N.I., Prosvirnin, S.L., 2008. Metamaterial analog of electromagnetically induced transparency. Phys. Rev. Lett. 101, 253903.

Quero, G., Consales, M., Severino, R., Vaiano, P., Boniello, A., Sandomenico, A., Ruvo, M., Borriello, A., Diodato, L., Zuppolini, S., Giordano, M., Nettore, I.C., Mazzarella, C., Colao, A., Macchia, P.E., Santorelli, F., Cutolo, A., Cusano, A., 2016. Long period fiber grating nano-optrode for cancer biomarker detection. Biosens. Bioelectron. 80, 590–600.

Rodrigo, D., Limaj, O., Janner, D., Etezadi, D., García de Abajo, F.J., Pruneri, V., Altug, H., 2015. Mid-infrared plasmonic biosensing with graphene. Science 349, 165–168.

Salim, A., Lim, S., 2018. Recent advances in the metamaterial-inspired biosensors. Biosens. Bioelectron. 117, 398–402.

Sun, H., Yin, L., Li, S., Han, S., Song, G., Liu, N., Yan, C., 2013. Prognostic significance of idh mutation in adult low-grade gliomas: a meta-analysis. Journal of Neuro-oncology 113, 277–284.

Tassin, P., Zhang, L., Zhao, R., Jain, A., Koschny, T., Soukoulis, C.M., 2012. Electromagnetically induced transparency and absorption in metamaterials: the radiating two-oscillator model and its experimental confirmation. Phys. Rev. Lett. 109, 187401.

Wallace, V.P., Fitzgerald, A.J., Pickwell, E., Pye, R.J., Taday, P.F., Flanagan, N., Ha, T., 2006. Terahertz pulsed spectroscopy of human basal cell carcinoma. Appl. Spectrosc. 60, 1127–1133.

Wei, Z., Li, X., Zhong, N., Tan, X., Zhang, X., Liu, H., Meng, H., Liang, R., 2017. Analogue electromagnetically induced transparency based on low-loss metamaterial and its application in nanosensor and slow-light device. Plasmonics 12, 641–647.

Xiao, S., Wang, T., Liu, T., Yan, X., Li, Z., Xu, C., 2018. Active modulation of electromagnetically induced transparency analogue in terahertz hybrid metal-graphene metamaterials. Carbon 126, 271–278.

Yan, X., Yang, M., Zhang, Z., Liang, L., Wei, D., Wang, M., Zhang, M., Wang, T., Liu, L., Xie, J., Yao, J., 2019. The terahertz electromagnetically induced transparency-like metamaterials for sensitive biosensors in the detection of cancer cells. Biosens. Bioelectron. 126, 485–492.

Yang, M., Liang, L., Zhang, Z., Xin, Y., Wei, D., Song, X., Zhang, H., Lu, Y., Wang, M., Zhang, M., Wang, T., Yao, J., 2019. Electromagnetically induced transparency-like metamaterials for detection of lung cancer cells. Opt Express 27, 19520–19529.

Yang, X., Zhao, X., Yang, K., Liu, Y., Liu, Y., Fu, W., Luo, Y., 2016. Biomedical applications of terahertz spectroscopy and imaging. Trends Biotechnol. 34, 810–824.

Yang, Y., Kravchenko, I.I., Briggs, D.P., Valentine, J., 2014. All-dielectric metasurface analogue of electromagnetically induced transparency. Nat. Commun. 5, 1–7.

Yu, C., Fan, S., Sun, Y., Pickwell-MacPherson, E., 2012. The potential of terahertz imaging for cancer diagnosis: a review of investigations to date. Quant. Imag. Med. Surg. 2, 33.

Zaha, D.C., 2014. Significance of immunohistochemistry in breast cancer. World J. Clin. Oncol. 5, 382.